Di-Electric Properties of Alzn Tio_3 and Alznni Tio_3 Nano Particles Using Sol-Gel Powder

Srinivasa S.[1], Dr. Vipin Kumar[2]

[1]Research Scholar, OPJS University, Churu, Rajasthan
[2]Professor, OPJS University, Churu, Rajasthan

Abstract

The sol-gel process produced nano-sized $ZnTiO_3$. TGA/DTA analysis, X-ray diffraction, TMA analysis, and scanning electron microscopy were all used to learn more about the nano particles. Sol-gel powders were found to have crystallized at 600 degrees Celsius, with crystallite diameters of 10 nm. The SEM analysis reveals that most of the $ZnTiO_3$ nano particles that were generated are clumped together. Sol was able to effectively produce ceramic nano-composites of (Al_2O_3/$BaTiO_3$). Data from experiments showed that when Al_2O_3 was added to $BaTiO_3$, the structure and particle size changed from tetragonal with 7e9 mm to orthorhombic with 400e600 nm. A very large peak may be seen in UV/Vi's spectra between 550 and 700 nm. Finally, the influence of Al2O3 nanoparticles on the dielectric characteristics as a function of temperature and frequency was studied. For their potential usage as Multilayer ceramic capacitors in electrical devices, the dielectric properties of the composites have been researched in great depth.

Keywords: - Dielectric Properties, Structure, Dielectric Tunability, Al2O3/BaTiO3, Permittivity

1. INTRODUCTION

With the proliferation of modern communication tools and electronic devices comes an increase in electromagnetic and microwave radiation pollutions. As a result, efforts are being made to develop materials that can block radiation and microwaves. Magneto plumbite hexaferrites are well suited for use as electromagnetic interference (EMI) suppressing and radar absorbent materials due to their low magnetic losses at gigahertz frequencies. You may categorize hexagons into six different types: M, W, X, Y, Z, and U. Complex hexaferrites may be built from structurally dissimilar S ($2MFe_2O_4$), R (Sr/Sr Fe_6O_{11}), and/or T ($(Ba/Sr)_2$ Fe_8O_{14}) blocks. However, their Gibbs free energy of synthesis and thermodynamic conditions for their production are identical. The stoichiometry of one Hexaferrite may lead to the formation of another Hexaferrite with a slightly different collection of structural blocks depending on the reaction mixtures utilized. X-type hexaferrites, which have low coercivity and high saturation magnetization, are among the most challenging to manufacture, but they are among the various varieties of hexagonal ferrites that are perfect for microwave absorption.

Multilayer ceramics are often regarded as a "smart material" for their applications in modern electronics, where they have been shown effective in the miniaturization of electrical circuitry in portable gadgets like smartphones, tablets, laptops, and desktops. To create them, alternating layers of ferrite and conducting electrode are coated and then co-fired. Ni-Cu-Zn ferrite has a high Curie temperature and electrical resistance, making it one of the most versatile magnetic materials for MLCls applications because of its great performance in the high frequency range and at low firing temperature. The ceramic capacitor used in electronics is a significant use of the oxide compounds. The dielectric ceramic substance serves as the insulator, while metal layers function as the electrodes in a ceramic capacitor. Different types of dielectric materials have different electrical properties and uses. For example, resonant circuits need low-loss, high-stability ceramic capacitors. This is only one of two types of ceramic capacitors. Second, the by-pass, buffer, and coupling applications all benefit greatly from the system's excellent volumetric efficiency. Multilayer ceramic capacitors (MLCCs) are utilized in a wide variety of electronic devices, and they are mass produced at a rate of around a trillion units each year. Because of its low capacitance, MLCCs are useful in op-amp, filter, and bypass circuits. Perovskite materials, such as manganite La0.70Sr0.30MnO2.85, are used in electronic devices due to their high quality physical and chemical properties, and the effects of magnetic fields and hydrostatic pressures on the magnetic properties and phase separation of perovskite materials have been studied by S.V. Trukhanov et al. But there's another group of oxide materials, including complex iron oxides, that show just as much promise for real-world use. Composites based on barium titanate (BaTiO3) have found use in the manufacture of multilayer ceramic capacitors (MLCCs), sensors, actuators, permittivity thermistors, etc. BaTiO3 has strong performance at high frequencies and is stable at high temperatures. BaTiO3 is well-known for being an eco-friendly, lead-free perovskite. The manufacturing of dielectric nanocomposites has improved as a result of the growth in sophistication of electronic devices.

UV/Vi's spectroscopy was used to investigate the optical qualities of the ceramic samples. Dielectric characteristics as a function of frequency and temperature were studied in relation to the amount of Al2O3 added to BaTiO3 (by %wt.). For their potential usage as multilayer ceramic capacitors (MLCCs), the composites' dielectric characteristics have been extensively researched.

2. LITERATURE REVIEW

Parida, Sabyasachi et.al. (2012) X-ray diffraction, Fourier transform-Raman spectroscopy, and Fourier transform-infrared spectroscopy were all used to study compositionally induced phase transitions in the system Sr (ZrxTi1x) O3. Two tilted phase transitions, pm3m-I4mcm and I4/mcm-pnma, were seen in the Sr (ZrxTi1-x) O3 system. BO6 octahedra tilted, causing the

structural transition. As the percentage of Zr increased, the dielectric constant measured using the Hakki-Coleman method dropped from 253 to 25. SrTiO3 had a value of 1771 ppm/°C for f, whereas SrZrO3 was only 82 ppm/°C. Experiments were conducted using a monopole antenna fed via an infinite ground plane, and simulations were run in Ansoft's high frequency structure simulator software to learn more about the dielectric resonator antenna (DRA). The composition between $0 \leq x \leq 1.0$.was studied to determine the necessary resonance frequency and bandwidth of DRA.

Giri, N et.al. (2018) Nano-crystalline samples of aluminum-doped zinc oxide (AZO) have been generated using the chemical precipitation process at varying doping concentrations. X-ray diffraction (XRD) and field emission scanning electron microscopy (FE-SEM) have been used for in-depth structural and morphological studies of Zn1-xAlxO. The effect of dopant concentration on the AZO particle size distribution has been investigated. Zn1-xAlxO (x 0.1) has its ac conductivity, dielectric constant, and dielectric loss studied in relation to both frequency (ω) and doping concentration (x) at room temperature.

A. A. Al-Ghamdi (2014) Glass substrates were successfully coated with aluminum doped ZnO (AZO) thin films using a spin coating process. X-ray diffraction, atomic force microscopy (AFM), and energy dispersive X-ray spectroscopy were all used to examine the films' structural characteristics. The X-ray diffraction analysis shows that all the films have a polycrystalline structure, and their preferred orientation is in the (002) plane, making them hexagonal wurtzites. Scherrer's formula and Williamson-Hall analysis were used to ascertain the crystallite size of ZnO and AZO films. Increasing the amount of Al in the AZO films was shown to cause a drop in the films' lattice properties. The AZO thin films include traces of Zn, Al, and O, as shown by energy dispersive spectroscopy (EDX). Increasing the amount of Al doped into the films increases their electrical conductivity, carrier mobility, and carrier concentration. Increasing the Al content raises the optical band gap (Eg) of the films. On average, the AZO thin films show 86% transparency in the visible spectrum. There is hope that these transparent AZO films may pave the way for novel optoelectronic and photonic device applications.

G.M. Rashwan et.al. (2021) (Ba0.95 Ca0.05) The solid-state reaction approach was used to make TiO3 ceramic at 1100°C, 1150°C, and 1200°C calcination temperatures. The results of an X-ray Diffraction (XRD) examination reveal that crystallization begins at a temperature of 1200 °C. Three hours were spent sintering at 1400 degrees Fahrenheit. The sample was analyzed using a UV-Visible spectrophotometer, a scanning electron microscope, and a transmission electron microscope. The highest dielectric constant () =1982 was determined by measuring the sample's dielectric characteristics between 25 and 140 degrees Celsius. Ca-ions replace Ba-ions in the tetragonal unit cell, preserving the perovskite's tetragonal structure, as determined by Rietveld refinement analysis of the XRD pattern.

3. RESEARCH METHODOLOGY

Sol-gel synthesis (sg-ZT)

Titanium butoxide (Ti (OC4H9)4) (purity 99.5%) was used in the synthesis of the ZnTiO3 gel. After stirring for 30 minutes, titanium butoxide was diluted in absolute ethanol (99.5% purity). A homogenous solution was prepared by adding the obtained solution drop by drop to a solution of ethanol, water, and a few drops of HNO3 and stirring the mixture for a further 2 hours (solution 1). Zinc acetate, Zn (OOCCH 3)2 (purity 99.5%), was similarly dissolved in ethylene glycol to make solution 2. After 1 hour of continuously stirring, solution 2 was slowly added to solution 1 in a drop-by-drop fashion, producing a uniform gel. The resulting gel was dried at 110 °C for 5 hours, then pulverized in a mortar to generate powder and heat treated in air for 2 hours at different temperatures (600 °C, 700 °C, 800 °C, 900 °C, and 1000 °C). Diagrammatic representation of the whole procedure is shown in Fig. 1.

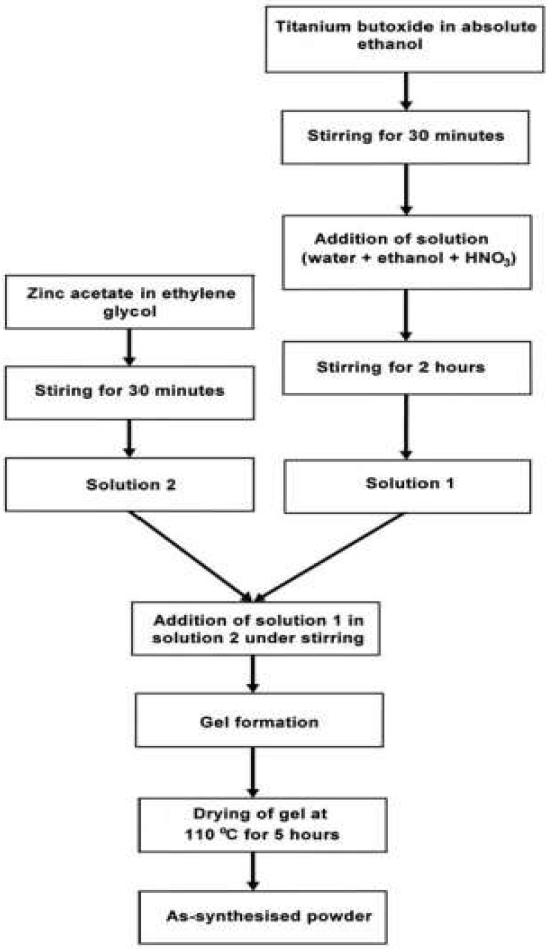

Figure 1. Schematic flow chart of the synthesis of $ZnTiO_3$ powders by sol-gel technique

Synthesis of Solids (ss-ZT) Both ZnO and TiO2 (purity >99%) were properly weighted to achieve the desired Zn/Ti = 1 molar ratio as the precursors. Zirconia balls were used to stir an ammonia solution with a pH of 11 for three hours in a Teflon container. It was found that these circumstances allowed for the most stable suspension to form. We then dried the slurry and reground the resulting powder by hand before subjecting it to a two-hour heat treatment in air at temperatures of 700°C, 800°C, 900°C, and 1000°C. In the end, the powder was reground in an ammoniac solution at pH = 11 for 1 hour.

Processing of ZnTiO3 ceramics

Uniaxial pressing (with a load of around 21 kN) of the synthesized powders combined with an organic binder (polyvinyl alcohol at 5 vol.%) yielded pressed pellets (8 or 6 mm in diameter and 2 mm thick). After two hours of heating and cooling at 150 °C/h, the green samples were sintered in air in a tubular furnace at a dwell temperature calculated by thermo-mechanical analysis.

Preparation of Al_2O3/BaTiO3 nanoparticles

Powders of BaCO3 (99.9% purity), TiO2 (99.99%), and Al2O3 (99.99%) were acquired from Al-Gomhouria Co., Ltd. (Cairo, Egypt). Sigma-Aldrich was sourced for the acetic acid used here. After combining a stoichiometric quantity of BaCO3 powder and TiO2 powder in a mortar for 30 minutes, the Sol. Gel. technique called for the powders to be suspended in a combination of 250 mL ethanol and 10 mL acetic by ultrasonication for 30 minutes at room temperature with magnetic stirring. Ammonia water solution was then added to bring the pH of the suspension to the desired level of 7. For a complete hydrolysis of BaTiO3, the resulting suspension was heated to 60 °C and held there for at least three hours with magnetic stirring. BaTiO3 solution was centrifuged and ethanol washed to finish the process.

Meanwhile, Al2O3 was suspended in 150 mL of methanol and 5 mL of acetic acid by ultrasonicating the liquid for 30 minutes with magnetic stirring at room temperature. In the meanwhile, an ammonia water solution was added to bring the pH level of the suspension up to 7. For a complete hydrolysis reaction of Al2O3, the resulting suspension was heated to 60 °C and kept there for 3 hours with magnetic stirring. The Al2O3 solution was then centrifuged and rinsed with methanol to remove any remaining particles.

1. DATA ANALYSIS

Sol-gel produced ZT powder TGA and DTA curves for the sol-gel powder (shown in Figure 2) provide evidence for the following events.

- On the DTA curve, we see an exothermic peak between 277 and 358°C, along with a weight loss of 20% (TGA curve). This is because the organic solvents have evaporated, and the organic remains have been broken down.
- As a consequence of the dihydroxylation of Ti-OH into TiO2, an exothermic peak is seen between 320 and 380 °C.
- It seems that all biological stuff is destroyed by the time temperatures reach 500 °C, therefore the weight loss stops at that point.

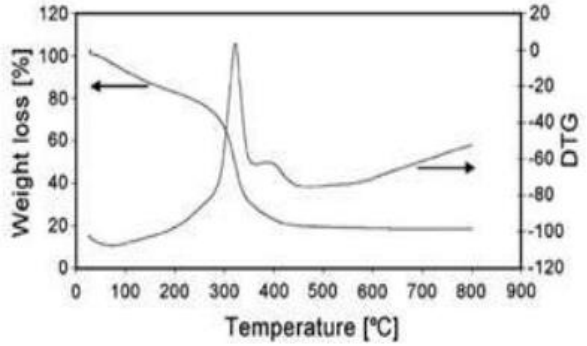

Figure 2. TGA-DTA curves of ZT gel precursor under air

Figure 3 shows the dilatometric curves for the powders. These tests were conducted on powders made from ssZT that had been annealed at 800 °C and sg-ZT that had been annealed at varying temperatures. Unlike ss-ZT, whose shrinkage is complete at 1150 °C, sg-ZT continues to shrink below this temperature.

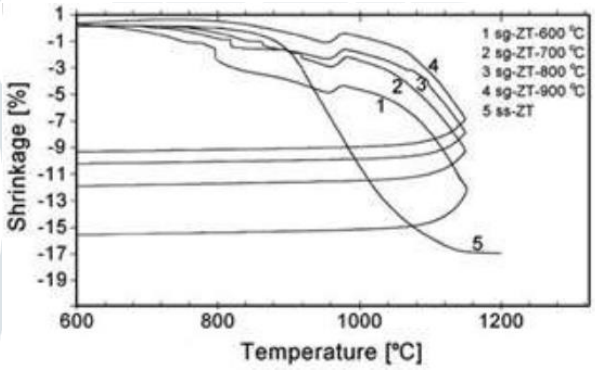

Figure 3. Shrinkage curves versus temperature of sg-ZT heat treated at different temperatures

UV/Vi's spectrometer

Ceramic samples of BaTiO3 and Al2O3/BaTiO3 were tested for their optical absorbance spectra in the region of 200-800 nm, as shown in Fig. 4. Specifically, BaTiO3 and Al2O3/BaTiO3 exhibit strong absorbance in the UV range but poor absorbance in the visible region. We find that the absorbance of BaTiO3 and Al2O3/BaTiO3 decreases with increasing wavelength, ranging from 0.060-0.027% in the shorter wavelength range. Band-to-band transfer between conduction bands and ionized acceptor is also demonstrated by a rise in absorbance upon adding Al2O3 to BaTiO3. With Al2O3, we see a blue shift and a change in the absorption edge toward shorter wavelengths. The semiconducting character of nanocomposites was revealed by the fact that their absorbance spectra were very sensitive to the amount of Al2O3 added to their surfaces, layers, and grain distributions. Also, the peak is rather prominent between 550 and 650 nanometers. Additive Al2O3 may have shown bands intermediate to those of valence and conduction. It might result from leakage current and free charges in the dielectric materials.

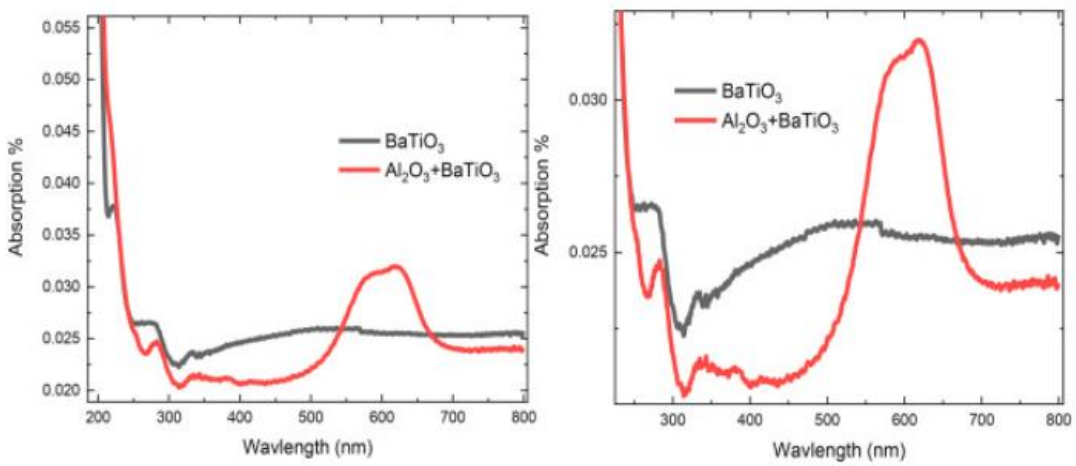

Fig. 4. UV/Vi's spectra of both $BaTiO_3$ and Al_2O_3/($BaTiO_3$) samples composites ceramics.

Dielectric properties

Information on dielectric qualities, such as electrical transport parameters, grain boundaries, and charge storage capacities, is very useful. There are several factors, such as the chemical make-up and manner of production, that affect its final form. Here, we looked at how the Al2O3/BaTiO3 composite changed in dielectric characteristics between 30 and 200 degrees Celsius and at frequencies of 20 to 10 megahertz. Fig.5 displays the experimental results for the real component of the dielectric constant (ε′). (a). As can be seen, the dielectric constant for Al2O3/BaTiO3 decreases linearly with increasing frequency, as is usual for BaTiO3. The weakening of the impact of space charge polarization is responsible for this drop. The rate of decrease in dielectric constant (ε′) is where the influence of Al2O3 becomes apparent. The existence of space charge polarization at the grain boundaries creates a potential barrier, which increases the dielectric constant at low frequencies. The real component of the permittivity then increased as a result of charge buildup at the grain boundary. Dielectric constant for Al2O3/BaTiO3 sample linearly decreases quicker at low frequencies f 1000 Hz. The dielectric constant is temperature invariant above 105 hertz. As frequency increased, the dielectric constant dropped from 106 to 100. In the high-frequency range (f > 105 Hz), the dielectric constant rapidly dropped with frequency and was found to be temperature-independent. Here, we have a flow explanation for the decrease in the real part of the dielectric constant at higher frequencies (f > 105); it is plausible to assume that the dielectric structure of Al2O3/BaTiO3 is made up of high conductive grains (Al2O3) separated by poor conducting thin grain boundaries (BaTiO3), resembling a capacitor. Due to interfacial polarization, an electric field caused charges to accumulate locally.

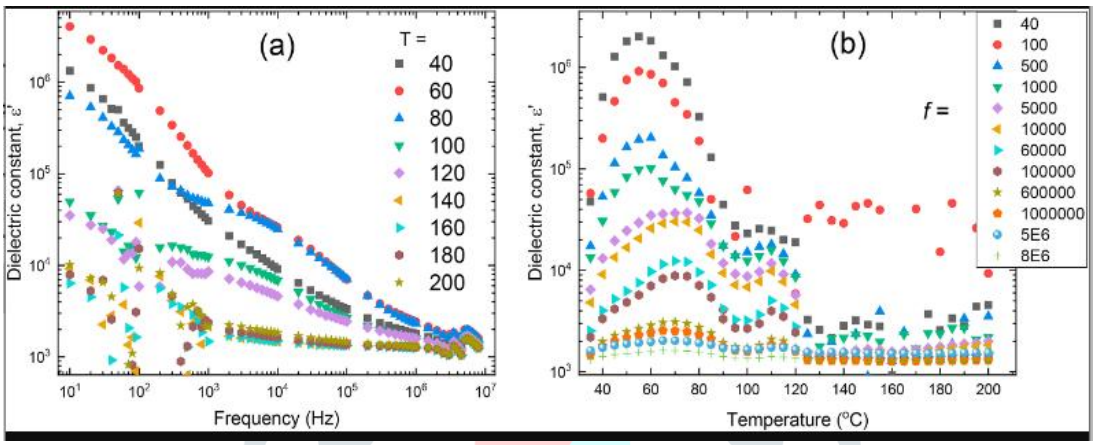

Fig.5. The dependence of dielectric constant of Al_2O_3/($BaTiO_3$) composites ceramics investigated as a function of frequency (10 Hz–10 MHz) at different temperatures (20–200 °C).

The dielectric constant (′) of Al2O3/BaTiO3 composites was measured as a function of temperature (30-200 °C) and frequency (Fig. 5(b)) (10 Hz–10 MHz). Dielectric constant (ε′) exhibits a large peak between 40 and 100 °C, then quickly drops to a lower value at roughly 115 °C. At about 110 degrees Celsius, BaTiO3 is known to undergo a phase shift from ferroelectric to paraelectric. BaTiO3 exhibits the expected behavior for its dielectric constant. More importantly, the frequency dependence of the dielectric constant is seen only for temperatures below T <100 °C, whereas at higher temperatures the dielectric constant is independent of temperature.

One may calculate the tangent of the dielectric loss, tan(δ), using an equation that relates it to the dielectric relaxation process.

$\tan(\delta) = \varepsilon'/\varepsilon''$

The dielectric loss, which occurs when the polarization lags behind the electric field due to grain boundaries, is a measure of the energy lost. Space charge migration (interfacial polarization contribution), molecule dipole motion, and direct current (DC) conduction are the three main causes of dielectric loss in insulator solids.

2. CONCLUSION

The low crystallization temperature (600 °C) and excellent purity of the sg-ZT powders were emphasized in this research as two major benefits of the sol-gel technique. Furthermore, the sg-ZT powders had a very tiny crystalline size. The powder, however, tended to clump together, which was a drawback. The ceramics' densification is negatively impacted by this process. Attrition milling was shown to be the most effective method of deagglomeration after tests were conducted on it, ultrasonication, and pulverization. Densifying the ceramic was simplified by the low agglomerate content of the sg- ZTattr powder. Furthermore, the UV/Vis spectrum reveals a massive peak between 550 -700 nm. Raman spectra reveals there is a peak at 900 nm and split for Al2O3/BaTiO3. Several peaks at a very low wave number (<900 cm1) were detected by the FT-IR and assigned to Al2O3/BaTiO3. Finally, the Al2O3/BaTiO3 nanoparticles had a significant impact on the temperature and frequency dependency of the dielectric characteristics. According to Koop's theory, the Maxwell-Wagner type of polarization may be used to explain the frequency- and temperature-dependent dielectric behavior of Al2O3/BaTiO3. BaTiO3's phase transition is also shown by the dielectric constants as a function of temperature.

3. REFERENCES

1. Parida, Sabyasachi & Rout, Sanjeeb & V, Subramanian & Barhai, P. K. & Gupta, Nisha & Gupta, Vibha. (2012). Structural Microwave Dielectric Properties and Dielectric Resonator Antenna studies of Sr(ZrxTi1-x) O3 ceramics. Journal of Alloys and Compounds. 528. 126-134. 10.1016/j.jallcom.2012.03.047.
2. Giri, N et.al. (2018) Structural and dielectric properties of Zn1−xAlxO nanoparticles Volume 1953, Issue 1 > 10.1063/1.5032666 https://doi.org/10.1063/1.5032666
3. Al-Ghamdi, O. A. Al-Hartomy and M. El Okr, Spectrochimica Acta Part A: Molecular and Biomolecular Spectroscopy 131, 512–517 (2014). https://doi.org/10.1016/j.saa.2014.04.020,
4. G.M. Rashwan, M. Mostafa, M.K. Gerges, A.A Ebnalwaleda, 2021 Preparation and Characterization and Dielectric Properties of (Ba0.95Ca0.05) TiO3 Ceramic Material Int. J. Thin. Film. Sci. Tec.10, No. 3 , 127-135 (2021) 1 Sep. 2021. Received: 11 Jan. 2021, Revised: 21 Feb. 2021, Accepted: 19 Mar. 2021. http://dx.doi.org/10.18576/ijtfst/100301
5. L. B. Kong, S. Li, T. S. Zhang, J. W. Zhai, F. Y. C. Boey, and J. Ma, “Electrically tunable dielectric materials and strategies to improve their performances,” Prog. Mater. Sci., 55(8), 840–893, 2010, doi: 10.1016/j.pmatsci.2010.04.004.
6. Priya, E. Sinha, and S. K. Rout, “Structural, optical and microwave dielectric properties of BaS_xSrxWO4 ceramics prepared by solid state reaction route,” Solid State Sci., 20, 40–45, 2013.
7. M. J. Gázquez, J. P. Bolívar, R. Garcia-tenorio, and F. Vaca, “A Review of the Production Cycle of Titanium Dioxide Pigment.,”. May, 441–458, 2014.
8. Q. Yue, L. Luo, X. Jiang, W. Li, and J. Zhou, “Aging effect of Mn-doped Ba0.77Ca0.23TiO3 ceramics,” J. Alloys Compd.,610,276–280,2014, doi: 10.1016/j.jallcom.2014.05.003.
9. Q. Zhang, J. Zhai, Q. Ben, X. Yu, and X. Yao, “Enhanced microwave dielectric properties of Ba0.4Sr0.6TiO3 ceramics doping by metal Fe powders,” J. Appl. Phys.,112(10), 104104, Nov. 2012, doi: 10.1063/1.4766276.
10. M. Mostafa, K. Ebnalwaled, H. A. Saied, and R. Roshdy, “Effect of laser beam on structural, optical, and electrical properties of BaTiO3 nanoparticles during sol-gel preparation,” J. Korean Ceram. Soc., 55(6), 581–589, 2018, doi: 10.4191/kcers.2018.55.6.04.
11. K. Momma and F. Izumi, “{\it VESTA3} for threedimensional visualization of crystal, volumetric and morphology data,” J. Appl. Crystallogr., 44(6), 1272–1276, 2011, doi: 10.1107/S0021889811038970.
12. G. M. R. M.K. Gerges, M. Mostafa, “Structural, optical and electrical properties of PbTiO3 nanoparticles prepared by Sol-Gel method,” Ijlret., 2(4), 42–49, 2016.
13. L. Cui, Y.-D. Hou, S. Wang, C. Wang, and M.-K. Zhu, “Relaxor behavior of (Ba,Bi)(Ti,Al)O3 ferroelectric ceramic,” J. Appl. Phys., 107(5), 54105, 2010, doi: 10.1063/1.3327244.
14. Aal, A. Abdel, et al. "FTIR study of nanostructure perovskite BaTiO3 doped with both Fe3+ and Ni2+ ions prepared by sol-gel technique." Acta Phys. Pol., A 126.6, 1318-1322, 2014.